Universal driving structure of self-sustained oscillatory complex networks

Xuhong Liao,[1][*] Weiming Ye,[1][*] Xiaodong Huang,[1] Qinzhi Xia,[1]

Xuhui Huang,[1] Pengfei Li,[1] Yu Qian,[1] Xiaoqing Huang,[1] Gang Hu[1][†]

[1]Department of Physics, Beijing Normal University,

Beijing 100875, China,

[*] These authors contributed equally to this work.

[†]To whom correspondence should be addressed; E-mail: ganghu@bnu.edu.cn

Recently, self-sustained oscillations in complex networks consisting of nonoscillatory nodes (network oscillators) have attracted great interest in diverse natural and social fields. Due to complexity of network behaviors, little is known so far about the basic structures and fundamental rules underlying the oscillations, not to mention the principles of how to control it. In this article we propose a common design principle for oscillations; predict novel and universal Branched Circle (BC) structures of oscillatory networks based on this principle; and suggest an operable Complexity Reduction Method to reveal the BC structures. These ideas are applied to excitable cell networks (including neural cell networks), and genomic regulatory networks. Universal BC structures are identified clearly in these two considerably different systems. These BC structures reveal for the first time both oscillation sources and wave propagation pathways of complex networks, and guide us to control the oscillations with surprisingly high efficiency.

1

Introduction

Self-sustained oscillations in complex networks consisting of non-oscillatory nodes are very popular phenomena in natural and social systems. These oscillations are extremely important in controlling various basic rhythms in wide fields, such as oscillatory neural networks (1–7), sinoatrial node rhythms in cardiac systems (8–10), oscillatory cycles in genomic regulations (11–17) and so on. Though the topic of self-sustained oscillations has been investigated for some decades, many fundamental questions remain in puzzle. For instance,we do not know whether there are some common principles underlying the oscillatory behaviors of complex networks in diverse fields; whether there are some common structures hidden in the complicated interaction schemes that determine the dynamics of oscillations; and if these common structures do exist, how one can find them. Specially, an given oscillatory networks as Figs. 1A, 1B, one can hardly say anything about where the oscillation sources are; how oscillatory waves propagate from the sources to the whole networks and how one can efficiently control the oscillations based on these understandings. None of these questions of crucial importance has been answered if networks are sufficiently complicated.

In this article we have made the following essential advances. (i) We start from a simple while solid basis design principle: any individually nonoscillatory node can oscillate if and only if it is driven by one or few interactions with advanced phases. (ii) Based on this design principle, all periodically oscillatory one-dimensional (1D) networks must have universal unidirectional coupling structures of branched circles (BCs, Fig. 2) in the form of circles with radiating branches. (iii) Oscillatory high-dimensional complex networks can be reduced to 1D BC networks by applying the method of dominant phase-advanced driving pathes.

We further apply the above ideas to both oscillatory excitable cell networks (ECNs, neural cell networks included) (5–7,18–20) and genomic regulatory networks(GRNs) (21–24). It's the first time the oscillations of these two considerably different systems are studied with a unified approach. We have reached the following results. (i) We apply the same design principle and dimension reduction approach to two kinds of systems and obtain the same universal BC structures; (ii) From the BC patterns of both systems we can clearly identify the oscillation sources (unidirectional regulatory circles) and reveal the phase propagation

pathways (unidirectional tree branches); (iii) With these BC patterns we can classify one or few most important nodes, by controlling which we can control the oscillations of the whole networks with surprisingly high efficiency.

Design principles and universal structures

Figure 1*A* considers an ECN example in which multiple cells with a large number of random couplings show a rather complicated interaction pattern. Although each individual node is nonoscillatory, with certain initial conditions we observe periodic oscillations, one of which is shown in Fig. 1*B*. We further study how sensitive the oscillation is to the control. After exhaustive tests we find that the oscillation can be terminated (i.e., turned to the homogeneous rest state $u_i = v_i = 0, i = 1, 2, .., N$) by removing a single red node (node 78) shown in Fig. 1*C*, while the oscillation persists safely if we remove as many as 70 empty square nodes in Fig. 1*C*. Here removing a node we mean to discard all interactions from and toward the given node. The results of Fig. 1*C* are highly surprising. They clearly show that though the topological interaction structure of Fig. 1*A* is random and homogeneous, the dynamic organization supporting self-sustained oscillation is strongly heterogeneous, and the roles played by different nodes in this organization are considerably different. The central task of the present work is to reveal these self-organized patterns under the conditions of full knowledge of coupling structure and output data and then to achieve an effective control of the oscillatory networks based on this understanding.

Considering a network with N nodes, dynamic variables are associated to each node, and these variables obey well defined coupled ordinary differential equations (ODEs). Each node is nonoscillatory individually while the entire complex networks are periodically oscillatory. Regardless of different dynamics and coupling forms for different systems, we propose a common design principle for such oscillatory networks.

Design principle: each nonoscillatory node can oscillate if and only if it is driven by one or few oscillatory interactions with advanced phases.

The definitions of "advanced phase" for different systems will be explained later. Let us first consider the simplest 1D oscillatory network with each node phase-advancedly driven

by one node only (networks with N nodes and N unidirectional interactions). Suppose an arbitrary node i_1 is phase-advancedly driven by a node i_2 via coupling, which is phase-advancedly driven by node i_3 in turn, and this successive unidirectional driving chain goes as $i_1 \leftarrow i_2 \leftarrow i_3 \leftarrow \cdots \leftarrow i_k \leftarrow \cdots$. Since N is finite we must come to a node i_q, $q \leq N$, which is driven by one of the previous nodes $i_1, i_2, ..., i_{q-1}$, say i_p $(p < q)$. Then a successive regulatory loop $i_p \leftarrow i_{p+1} \leftarrow \cdots \leftarrow i_q \leftarrow i_p$ is formed, serving as the oscillation source of all other nodes. Therefore, all 1D oscillatory networks must have the structure of circles with radiating branches, schematically shown in Fig. 2.

The pattern of Fig. 2 gives a picture of a branched circle (BC), and it is thus called as BC structure. This structure is universal for self-sustained periodic oscillations in 1D networks consisting of nonoscillatory nodes. Since no nonoscillatory node oscillates without phase-advanced driving from other nodes, two key rules must be obeyed by any BC structure:

(i) There must be few (at least one) successively phase-advanced driving circles.

(ii) Each node not in the circles must be in a tree branch rooted at a node in a circle.

The BC circle is obviously the oscillation source without which the network can never oscillate, and the tree branches show various pathways of phase propagations starting from different circle nodes. All nodes in Fig. 2 can be classified according to their locations in the BC pattern. We expect that the circle nodes controlling large branches may be of the most importance for the oscillation. In comparison all nodes near the branch ends with few or even without downstream nodes have the lowest influences on the oscillation of the network. We will show later that these expectations are well confirmed by numerical results with large probability.

The simple and instructive scheme of Fig. 2 is deduced in 1D phase-advanced driving networks. However, interaction structures of complex networks in general (e.g., Fig. 1A which are high-dimensional and random) are much more complex than Fig. 2. Therefore, we propose an operable and physically meaningful method to reduce original random patterns (as Fig. 1A) to the simple and instructive BC pattern of Fig. 2. The method consists of the following Complexity Reduction (CR) steps:

(a) Find phase-advanced driving interactions for each node.

(b) Find the single dominant interaction among these phase-advanced driving interac-

4

tions.

(c) Use all these dominant interactions to unidirectionally link the network nodes, and draw the dominant phase-advanced path pattern, which turns out to be the 1D BC pattern of Fig. 2.

All the above steps are generally applicable in diverse fields for self-sustained oscillations of complex networks of individually nonoscillatory nodes. The particular meanings of "advanced phase" and "dominant phase-advanced driving" should be properly defined, according to realistic physical, chemical and biological interaction mechanisms in each individual system.

Coupled excitable cell networks

We now consider complex excitable cell networks (ECNs) of the Bär Model(18)

$$
\frac{du_i}{dt} = \frac{1}{\varepsilon} u_i (1 - u_i)(u_i - \frac{v_i + b}{a}) + D_u \sum_{j=1}^{\nu} (u_{ij} - u_i) ,
$$

$$
\frac{dv_i}{dt} = f(u_i) - v_i, \qquad i = 1, 2, ..., N \tag{1}
$$

$$
f(u_i) = \begin{cases} 0 & u_i \leq \frac{1}{3} , \\ 1 - 6.75 u_i (u_i - 1)^2 & \frac{1}{3} < u_i < 1 , \\ 1 & u_i > 1 . \end{cases}
$$

in which u_{ij} means the variable u of the jth node linked to node i. Note, two major features of neural networks are precisely the excitability of cell dynamics and the complexity of interaction network(20,25–27). Without couplings all cells of ECNs are not oscillatory individually for certain given a, b, they evolve asymptotically to the rest state $u = v = 0$ and will stay there forever unless some external force drives them from this state. Therefore, all the analyses in the former section are applicable to this type of systems. Whenever a cell is kicked from the rest state by a small stimulus, the cell can oscillate by its own internal dynamics (so called excitable dynamics). Therefore, for a given node that enters the region of the rest state ($u < u_{th}$) at time t_s and departs from this region at time t_e, we define "phase-advanced drivings" by the interactions from those neighbors which leave from

5

the rest state earlier than the given node (i.e., in the period (t_s, t_e)) which thereby provide favorable interactions in kicking the given cell from the rest state. Among these phase-advanced interactions the dominant phase-advanced driving is defined by the interaction from the node first leaving from the rest state in the period (t_s, t_e). It is no doubt that the dominant driving must give the most important contribution to excite the given node, i.e., to drive the given node to oscillate.

For simplicity, we assume symmetric couplings, and adopt random complex networks with identical coupling degree ν (i.e. each cell couples to equal number ν of other cells). We also take identical parameters for all cells. One advantage of this simplest homogeneous assumption is to make sure that all self-sustained oscillatory behaviors here are not due to any heterogeneity in topological structure, but due to the self-organized heterogeneity of dynamical mutual excitations.

Figure 1A shows an ECN with random mutual couplings with identical degree $\nu = 4$. With the structure of Fig. 1A we simulate the system by taking different sets of random initial conditions. In most of cases the system evolves asymptotically to the homogeneous rest state. However, about 8% of tests provide periodic oscillations, and the state in Fig. 1B is one of them.

In Fig. 3A we plot the BC pattern draw from Figs. 1A and 1B by applying the CR method. We find a BC pattern being the type of Fig. 2. In Fig. 3A the BC circle plays the role of oscillation source, and phase waves propagate down all the tree branches rooted at various cells in the circle. The BC structure of Fig. 3A clearly shows distinctive levels of significances of different cells for oscillation that cannot be observed in Fig. 1A. In Fig. 1A all cells stand equivalently in the homogeneous and randomly coupled network, and no cell takes any priority over others from the topological structure. The situation in Fig. 3A is different. Cells in the circle and cells in various turning points of large branches (which control large numbers of downstream cells) are likely to be important to the oscillation. In particular, node 78 is likely to be the most important cell because it locates in the circle on one hand and controls large branches with a huge number of downstream nodes on the other hand. It is interesting to observe that node 78 is the very single red node in Fig. 1C that we found important for controlling the oscillation but did not know the reason then.

In Fig. $3B$ we show how the oscillation collapses quickly to the homogeneous rest state after removing only a single red node 78. On the other hand, cells near the branch ends may be much less significant for the oscillation. We remove simultaneously a large number of cells (70 nodes) in branch tails (See Fig. $3C$) which are exactly the empty square nodes in Fig. $1C$, the network not only continues its periodic oscillation (Fig. $3D$), but also keeps the BC structure almost unchanged for the cells remained (Fig. $3C$). Therefore, the question for Fig. $1C$, why so many empty square nodes together are much less important than a single red cell, is clearly answered in Fig. $3A$: because all these empty square nodes are far from the centered oscillation generator, and have little influence on the self-sustained oscillation; on the other hand the single red cell 78 controls the oscillation source and a huge number of downstream nodes, and it is of crucial importance for the given oscillation. Removing one or few other cells in the circle may not stop the oscillation but can considerably change the BC structure of the oscillation source.

Frequency is an important quantity describing the properties of oscillatory networks. We further study the influence of BC circles on frequencies of networks. We computed Eqs. (1) by taking different random couplings and random initial conditions for $N = 100$, $\nu = 3$, and found some oscillatory realizations (all are periodic), we then measured the frequency ω of each oscillatory network, and plot ω vs n in Fig. 3E with n being the size of the corresponding circle. The red square represents the average frequency $< \omega >$ and the solid line denotes the linear fitting of the tendency. In Fig. 3E monotonous and nearly linear decrease of $< \omega >$ with n is clearly demonstrated. These observations convincingly support the conclusion that BC circles play the role of oscillation sources in complex networks.

Figure. $4A$ is another ECN network with $N = 100$ and $\nu = 3$. For certain initial condition, we observe periodic oscillation of Fig. $4B$. In Fig. $4A$ we show that this oscillation can be terminated by removing a pair of nodes (red nodes 12 and 21) in contrast with Fig. $1C$ where oscillation can be suppressed by removing only a single node. Similar to Fig. $1C$ oscillation persists when we simultaneously remove all 60 empty square nodes shown in Fig. $4A$. The mystery difference between Figs. $1C$ and $4A$ can be again well explained by the corresponding BC patterns. In Fig. $4C$ we show the BC pattern corresponding to the oscillation in Figs. $4A$ and $4B$. The essential and interesting difference between Fig. $3A$ and Fig. $4C$ is that Fig.

$4C$ contains two BC clusters instead of the single one in Fig. $3A$. The two red nodes shown in the two BC circles of Fig. $4C$ are exactly identical to those in Fig. $4A$ with the same color. Comparing the BC patterns of Fig. $4C$ with Fig. $3A$, we understand the difference of Fig. $1C$ and Fig. $4A$ immediately. Since there are two oscillation source circles in Fig. $4C$, we have to destroy both circle structures for terminating oscillation by removing two key nodes in Fig. $4A$ simultaneously, each from a circle of Fig. $4C$, and this is sharply different from the single circle structure of Fig. $3A$. In Figs. $4D$ and $4E$ we get the BC patterns with one of the two red nodes (node 12 and node 21) removed, respectively. It's interesting to see that in both cases one BC circle of Fig. $4C$ is destroyed while the other remained circle serves as the unique oscillation source, and all nodes of the destroyed BC cluster are engrafted to the survival circle for continuing their periodic oscillations. In Fig. $4F$ we remove 60 side cells (the empty nodes) simultaneously from Fig. $4C$, and find again that periodic oscillation persists, and the corresponding BC pattern of the unremoved nodes are not affected. We have tested a number of different ECNs with different initial conditions, different interaction degree and structures, different system sizes, or different ECN models including FHN neural cell networks, and obtained very rich behaviors of BC patterns. The general conclusions of universal BC patterns are verified in all cases, and some of these results are shown in Supporting Information Part 1.

Complex genomic regulatory circuits

We now consider another model of self-sustained oscillations of genomic regulatory networks (GRN), the dynamics is described by the following coupled ODEs(21–24).

$$
\frac{dx_i}{dt} = \mu_i - \gamma_i x_i + f_i, \quad f_i = \begin{cases} A_i(\boldsymbol{x}) & \text{Positive regulation ,} \\ R_i(\boldsymbol{x}) & \text{Negative regulation ,} \\ A_i(\boldsymbol{x})R_i(\boldsymbol{x}) & \text{Joint regulation ,} \end{cases}
$$

$$
\boldsymbol{x} = (x_1, x_2, \ldots, x_N) , \tag{2}
$$

$$
A_i(\boldsymbol{x}) = \frac{act_i^{h_i}}{act_i^{h_i} + K_i^{h_i}} , \quad R_i(\boldsymbol{x}) = (1 - \mu_i)\frac{K_i^{h_i}}{rep_i^{h_i} + K_i^{h_i}} ,
$$

$$act_i = \sum_{j=1}^{N} \alpha_j^{(i)} x_j \ , \quad rep_i = \sum_{j=1}^{N} \beta_j^{(i)} x_j \ , \quad (i,j = 1,\ldots,N) \ ,$$

where x_i represents the concentration of protein corresponding to node i, and act_i (rep_i) represents the summation of activatory (repressive) transcriptional factors. These ODEs can be derived from a full set of equations of both mRNA and potein concentrations via adiabatic approximation when the time scales of transcription and translation are separable(11). For simplicity we consider homogeneous parameter distributions again for all nodes ($\mu_i = \mu$, $\gamma_i = \gamma$, $h_i = h$, $K_i = K$, $\alpha_i = \beta_i = 1$, $i = 1, 2, \ldots, N$). It's emphasized that the GRN dynamics Eqs. (2) is apparently different from ECN Eqs. (1) for their intrinsic node dynamics (one-variable passive dynamics for Eqs. (2) against two-variable excitable dynamics for Eqs. (1)), coupling dynamics (highly nonlinear positive or negative regulatory interactions for Eqs. (2) while linear and diffusive coupling for Eqs. (1)), and coupling structure (unidirectional couplings for Eqs. (2) against symmetric couplings for Eqs. (1)). It is a surprise for us to observe essentially the same dynamic BC structures in both GRN and ECN systems as shown in the following.

Each node in Eqs. (2) has passive dynamics. Without coupling, variable x_i must evolve to a fixed value, and any periodic oscillation of x_i must be driven by one or few periodic interactions from other nodes. Let us approximately simplify an arbitrary one-variable passive dynamics with a periodical driving $\dot{x} = \mu - \gamma x + f(x,t)$ by linearizing the oscillatory elements around a stable stationary solution of the autonomous dynamics

$$\triangle \dot{x} = -\lambda \ \triangle x + A \cos(\omega t) \ , \tag{3}$$

which has the asymptotic periodic motion

$$\triangle x(t) = \frac{A}{\sqrt{\lambda^2 + \omega^2}} \ cos(\omega t - \phi) \ ,$$

$$sin\phi = \frac{\omega}{\sqrt{\lambda^2 + \omega^2}} \ , \quad cos\phi = \frac{\lambda}{\sqrt{\lambda^2 + \omega^2}} \ , \tag{4}$$

leading to the phase-advanced driving condition of

9

$$0 \lesssim \phi \lesssim \frac{\pi}{2} \ . \tag{5}$$

We represent the phase of node i by ϕ_i and the phase of interaction from node j to node i by $\phi_{j \to i}$, which is identified by

$$\phi_{j \to i} = \begin{cases} \phi_j & \text{positive regulation} , \\ \\ \phi_j + \pi & \text{negative regulation} . \end{cases} \tag{6}$$

The condition of phase-advanced driving reads

$$0 \lesssim \phi_{j \to i} - \phi_i \lesssim \frac{\pi}{2} \ . \tag{7}$$

With interaction structures and full periodic oscillation data of complex GRN known we can use Eqs. (6) and (7) to identify all phase-advanced interactions among all interactions (CR method (a)). To operate the CR method (b) we simply define the dominant driving by the interaction among all phase-advanced interactions which has the largest oscillation amplitude. The detailed discussion on the phase and amplitude computation is given in Supporting Information Part 2. After choosing the dominant interactions for various nodes, we can link all nodes by the dominant interactions and construct BC patterns from the original GRNs.

It is known that a necessary condition for a genomic regulatory loop to be oscillatory is that the genes in the loop must interact successively in a manner of negative feedback(13,21–24), i.e., the number of negative couplings should be odd(13,22). We call a successive uni-directional interaction loop with an odd number of negative interactions as an oscillatory negative feedback loop(NFL)(28) in the following. Note, existence of one or multiple oscillatory NFLs is the necessary but not sufficient condition of oscillatory networks. In Supporting Information Part 2 (Fig. S5), we show these oscillatory NFLs for $q \leqslant 5$. Nevertheless, given a complex network (e.g., Fig. 5D or 5E), there may exist a huge number of possible oscillatory NFLs. There is so far no report of a method to find out which NFLs are in function to produce a given oscillatory pattern. And this is right our following task.

In order to examine the validity of the general prediction on universal oscillatory BC patterns we have computed huge number of GRNs by varying dynamic parameters (homogeneous and heterogeneous), changing autoregulatory dynamics (with or without autoregulation, with negative or positive autoregulation); changing the number of nodes and the structure of couplings and also by varying the initial variable preparations. Specifically, we have made 328400 tests (about 1400 oscillatory realizations) by exhaustively computing different coupling structures of 3-node circuits; 10^4 random tests for 4-node and 5-node circuits (totally 2×10^4 tests, 708 oscillations); 5×10^3 random tests for 10-node and 20-node circuits (totally 1×10^4 tests, about 1083 oscillations), we found that none of the tests violates the predictions. In particular, we found that in all oscillatory cases we can succeed in constructing BC patterns all of which have circles being one of the oscillatory NFLs in Fig. S5. In Figs. 5A-E we show some periodically oscillatory examples of regulatory networks. Although the complicated interaction structures don't disclose any clue of the mechanism supporting the oscillations, by applying CR method we succeed in reducing the original complex networks to the corresponding BC patterns greatly simplified in Figs. 5F-J, respectively, which fully confirm the prediction of Fig. 2. Each BC pattern in Fig. 5 has a source circle being one of the oscillatory NFLs in Fig. S5, and all other nodes are in various tree branches rooted at one of circle nodes, showing wave propagation pathways.

From Figs. 5F-J we expect that the nodes in the circles or near the circles may be important for the given oscillatory states while nodes near the ends of various branches may be less significant. We study each gene's influence on oscillations by removing it. In Figs. 5F-J any node whose individual removal results in the termination of the oscillations are filled with red color, and empty otherwise. We find that by removing a gene on a circle we have very large probability to terminate the oscillation. However, when we remove a node located at the end of a branch pathway oscillations have much larger probability to persist. For statistics we have made a detailed investigation for 10-node oscillatory GRNs, and found that if we remove an arbitrary single node on BC circles the probability to terminate oscillations is about 84% while this probability is down to about 24% if an arbitrary single node on branches is removed.

For identifying the system response to control, we study the dynamic behavior of $N = 20$

(Fig. 5I) in more detail. In Fig. 6A we show oscillation of $< x(t) >= \frac{1}{N} \sum_{i=1}^{N} x_i(t)$ damping to a fixed value after a key circle node removed at $t = 1000$. On the other hand, the oscillation persists (Fig. 6B) and the BC structure is only slightly modified (Fig. 6C) as a node at a branch end is removed. Most interestingly, whenever self-sustained oscillations are maintained after removing some nodes, the BC circles have a strong tendency to be unchanged (Fig. 6C) or slightly modified by refinding some interaction bridges to repair the circles (Fig. 6D). All these observations verify the significance of the universal BC structures for oscillations of complex networks.

In Eqs. (2) we assume "AND" role between activators and repressors for multiple-factor regulations(21). Some regulatory circuits may obey "OR" role(11,23,29). Though the coupling dynamics of "OR" rule looks considerably different from Eqs. (2), all analyses for Eqs. (2) can be identically applied to the "OR" cases. This aspect is discussed in Supporting Information Part 3.

Discussion

In conclusion we study the problem of self-sustained periodic oscillations in complex networks consisting of nonoscillatory nodes. We propose a general design principle of oscillatory networks, based on which we reveal that phase-advanced driving BC patterns (Fig. 2) are the universal structures of simplest 1D oscillatory networks. And complicated high-dimensional networks can be reduced to these 1D BC patterns by applying the method of dominant phase-advanced interactions. From the BC patterns we can easily identify oscillation sources and phase propagation pathways of oscillatory complex networks. All these messages are deeply hidden in the original complex coupling structures and random phase distributions. These BC structures are extremely important for understanding and efficiently controlling self-sustained oscillations of complex systems. We successfully used these ideas and methods to analyze models of excitable cell networks and genomic regulatory circuits. These ideas, methods and universality of structures are expected to be applicable to self-sustained oscillations of complex networks in broad range of fields. In recent decades, the concept and functions of central pattern generators (CPGs) have attracted great attention in the field of

12

neural networks(30–33). In this article we show for the first time how to uncover CPG-like patterns in periodically oscillatory complex networks from complicated interaction structures and seemingly mess phase distribution data.

In the present article we consider only cases of periodic oscillations where all BC patterns are stationary. If oscillations are quasiperiodic or even chaotic, BC patterns may vary during the evolutions, and this opens a new field for the further study. Moreover, throughout this article we study how to reveal BC patterns with full knowledge of the interaction structures and oscillation data. These conditions are not fulfilled in many experiments. Thus, it is another crucial task to extend the investigations to the cases with partial data available.

References

[1] Buzsáki G, Draguhn A (2004) Neuronal oscillations in cortical networks. *Science* 304:1926-1929.

[2] Sanchez-Vives M V, McCormick D A (2000) Cellular and network mechanisms of rhythmic recurrent activity in neocortex. *Nature Neurosci.* 3:1027-1034.

[3] Steriade M, Timofeev I (2003) Neuronal plasticity in thalamocortical networks during sleep and waking oscillations. *Neuron* 37:563-576.

[4] Selverston A I, Moulins M (1985) Oscillatory neural networks. *Ann. Rev. Physiol.* 47:29-48.

[5] Lewis T J, Rinzel J (2000) Self-organized synchronous oscillations in a network of excitable cells coupled by gap junctions. *Network: Comput. Neural Syst.* 11:299-320.

[6] Sinha S, Saramäki J, Kaski K (2007) Emergence of self-sustained patterns in small-world excitable media. *Phys. Rev. E* 76:R015101.

[7] Roxin A, Riecke H, Solla S A (2004) Self-sustained activity in a small-world network of excitable neurons. *Phys. Rev. Lett.* 92:198101.

[8] Irisawa H, Brown H F, Giles W (1993) Cardiac pacemaking in the sinoatrial node. *Physiol. Rev.* 73:197-227.

[9] Boyett M R, Honjo H, Kodama I (2000) The sinoatrial node, a heterogeneous pacemaker structure. *Cardiovasc. Res.* 47:658-687.

[10] Mandel W, Hayakawa H, Danzig R, Marcus H S (1971) Evaluation of sino-atrial node function in man by overdrive suppression. *Circulation* 44:59-66.

[11] Tsai T Y C, *et al.* (2008) Robust, tunable biological oscillations from interlinked positive and negative feedback loops. *Science* 321:126-129.

[12] Pomerening J R, Kim S Y, Ferrell J E, Jr (2005) Systems-level dissection of the cell-cycle oscillator: bypassing positive feedback produces damped oscillations. *Cell* 122:565-578.

[13] Elowitz M B, Leibler S (2000) A synthetic oscillatory network of transcriptional regulators. *Nature* 403:335-338.

[14] Glossop N R J, Lyons L C, Hardin P E (1999) Interlocked feedback loops within the drosophila circadian oscillator. *Science* 286:766-768.

[15] Hirata H,*et al.* (2002) Oscillatory expression of the bHLH Factor Hes1 regulated by a negative feedback loop. *Science* 298:840-843.

[16] Geva-Zatorsky N, *et al.* (2006) Oscillations and variability in the p53 system. *Mol. Syst. Biol.* 13:msb4100068E1.

[17] Rust M J, Markson J S, Lane W S, Fisher D S, O'Shea E K (2007) Ordered phosphorylation governs oscillation of a three-protein circadian clock. *Science* 318:809-812.

[18] Bär M, Eiswirth M (1993) Turbulence due to spiral breakup in a continuous excitable medium. *Phys. Rev. E* 48:R1635.

[19] Jahnke W, Winfree A T (1991) A survey of spiral-wave behaviors in the Oregonator model. *Int. J. Bifur. Chaos* 1:445–466.

[20] Fitzhugh R (1961) Impulses and physiological states in theoretical models of nerve membrane. *Biophys. J.* 1:445-466.

[21] Ishihara S, Fujimoto K, Shibata T (2005) Cross talking of network motifs in gene regulation that generates temporal pulses and spatial stripes. *Genes to Cells* 10:1025-1038.

[22] Pigolotti S, Krishna S, Jensen M H (2007) Oscillation patterns in negative feedback loops. *PNAS* 104:6533-6537.

[23] Li C, Chen L, Aihara K (2006) Stability of genetic networks with sum regulatory logic: Lur'e system and LMI approach. *IEEE Trans. Cir. Sys.* 53:2451-2458.

[24] Mangan S, Zaslaver A, Alon U (2003) The coherent feedforward loop serves as a sign-sensitive delay element in transcription networks. *J. Mol. Biol.* 334:197-204.

[25] Hodgkin A L, Huxley A F (1952) A quantitative description of membrane current and its application to conduction and excitation in nerve. *J. Physiol.* 117:500-544.

[26] Izhikevich E M (2000) Neural excitability, spiking and bursting. *Int. J. Bifur. Chaos* 10:1171-1266.

[27] Izhikevich E M (2004) Which model to use for cortical spiking neurons. *IEEE Trans. on Neural Networks* 15:1063-1070.

[28] Alon U (2007) Network motifs: theory and experimental approaches. *Nature Rev. Genet.* 8:450-461.

[29] Buchler N E, Gerland U, Hwa T (2003) On schemes of combinatorial transcription logic. *PNAS* 100:5136-5141.

[30] Grillner S, Wallen P (1985) Central pattern generators for locomotion, with special reference to vertebrates. *Ann. Rev. Neurosci.* 8:233-261.

[31] Marder E, Bucher D (2001) Central pattern generators and the control of rhythmic movements. *Curr. Biol.* 11:R986-R996.

[32] Kiehn O, Butt S J B (2003) Physiological, anatomical and genetic identification of CPG neurons in the developing mammalian spinal cord. *Prog. Neurobiol.* 70:347-361.

[33] Yuste R, MacLean J N, Smith J, Lansner A (2005) The cortex as a central pattern generator. *Nature Rev. Neurosci.* 6:477-483.

Fig. 1. A complex excitable cell network of Eqs. (1) consisting of $N = 100$ nodes. $a = 0.84$, $b = 0.07$, $\varepsilon = 0.04$. All these parameters will be used in Figs. 1, 3, 4. All couplings with strength $D_u = 0.2$ are randomly chosen between N nodes each having coupling degree $\nu = 4$. *(A)* An example of network interaction structure. *(B)* Periodic orbit of average variables $< u(t) > = \frac{1}{N}\sum_{i=1}^{N} u_i(t)$ and $< v(t) > = \frac{1}{N}\sum_{i=1}^{N} v_i(t)$ of the network (A) for a set of initial conditions randomly chosen. *(C)* Oscillation of (B) can be terminated by removing a single red node. By removing a node we mean to discard all interactions from and towards the given node. However, oscillation persists if we simultaneously remove other 70 empty square nodes.

Fig. 2. Schema of universal structure of self-sustained oscillatory 1D networks with all nodes nonoscillatory individually. The arrowed lines indicate unidirectional phase-advanced interactions. Characteristic features are: one or few unidirectionally interacting circles serving as the oscillation sources together with unidirectionally interacting branches radiated from the circle showing wave propagation pathways (called branched circles, BC).

Fig. 3. BC patterns and their oscillation dynamics of ECNs. *(A)* BC pattern of Eqs. (1) reduced from Figs. 1(A) and 1(B) by applying CR method. From this pattern we are able to identify oscillation source (the unidirectional circle) and wave propagation pathways (the tree-like branches from various nodes of the circle). Self-sustained oscillation of Fig. 1(B) can be effectively suppressed by removing only a single red node 78, which is the same as that in Fig. 1(C). *(B)* Oscillation suppression by removing node 78 at $t = t_D = 10$. *(C)* BC pattern drawn after removing simultaneously the 70 empty square nodes shown in Fig. 1(C). Oscillation is kept and the BC pattern of the remaining nodes is not affected. *(D)* Oscillation evolution with 70 empty square nodes of (C) removed at $t = t_D = 10$, simultaneously. *(E)* Frequency ω of a periodic complex network of Eqs. (1) plotted vs the size n of the BC circle. Large red square represents the average frequency $< \omega >$, and solid line is the linear fitting of the data. $N = 100$, $\nu = 3$, $D_u = 1.0$. Coupling structures and initial conditions are randomly chosen. A strong correlation between $< \omega >$ and n is demonstrated by the monotonously decreasing curve.

Fig. 4. Manipulations of oscillatory complex networks. *(A)* Another ECN network with $N = 100$, $\nu = 3$, $D_u = 1.0$. *(B)* Oscillatory orbits of network (A) with a certain set of initial

condition. Oscillation persists after all the 60 empty square nodes shown in (A) are removed simultaneously. Apparently different from Fig. 1(C), now removing any single node can no longer terminate the oscillation. Oscillation can be suppressed by, at least, removing the pair of red nodes in (A). The difference between Figs. 1(C) and 4(A) is again an interesting mystery. *(C)* BC pattern of the oscillation in (B) considered. Now we find two separated BC clusters from two circles. Removing the pair of red nodes 12 and 21 can break the two source circle and terminate the oscillation. *(D)* BC pattern with a single node 12 removed. Now one BC circle with node 12 is destroyed and the remained circle of (C) plays the role of the unique oscillation source. *(E)* BC pattern with node 21 removed. *(F)* BC pattern after removing 60 side nodes from (C) (i.e., the 60 empty square nodes in (A)).

Fig. 5. Complex oscillatory GRNs and the corresponding BC patterns. The solid green (red dashed) line denotes positive (negative) regulation. The lines in the following figures on GRNs have the same meanings throughout the article. *(A)-(E)* Some examples of 4-node ($I = 9$ interactions), 6-node ($I = 20$), 10-node ($I = 55$), 20-node ($I = 105$), 40-node ($I = 224$) GRNs , respectively. $\mu_i = \mu = 0$, $\gamma_i = \gamma = 0.1$, $h_i = h = 2$, $K_i = K = 0.3$, $\alpha_i = \beta_i = 1$, $i = 1, 2, \ldots, N$. With the given interaction structures all these circuits show self-sustained periodic oscillations with arbitrary initial conditions. *(F)-(J)* BC patterns constructed from the periodic oscillation of networks of (A)-(E), respectively, by applying CR method. In all cases we find that each BC circle is one of the oscillatory NFLs in Fig. S5. A node whose individual removal terminates the oscillation is filled with red, otherwise it is empty.

Fig. 6. Detailed numerical results of Eqs. (2) for the case of Figs. 5(D) and 5(I) ($N = 20$). *(A)* Time evolution of the average concentration $< x >$, which periodically oscillates for $t \leqslant t_D$ and collapses to a stationary solution after we remove a circle node 15 at $t_D = 1000$. *(B)(C)* Time evolution and BC pattern , respectively, with node 6 removed at $t_D = 1000$. The BC circle of Fig. 5(I) is not changed by removing this branch gene. *(D)* BC pattern with node 18 removed. In (D) the BC circle must be changed by removing a circle gene, however, the system repairs the broken circle by finding some interaction bridges with most of original circle nodes kept on the new circle.
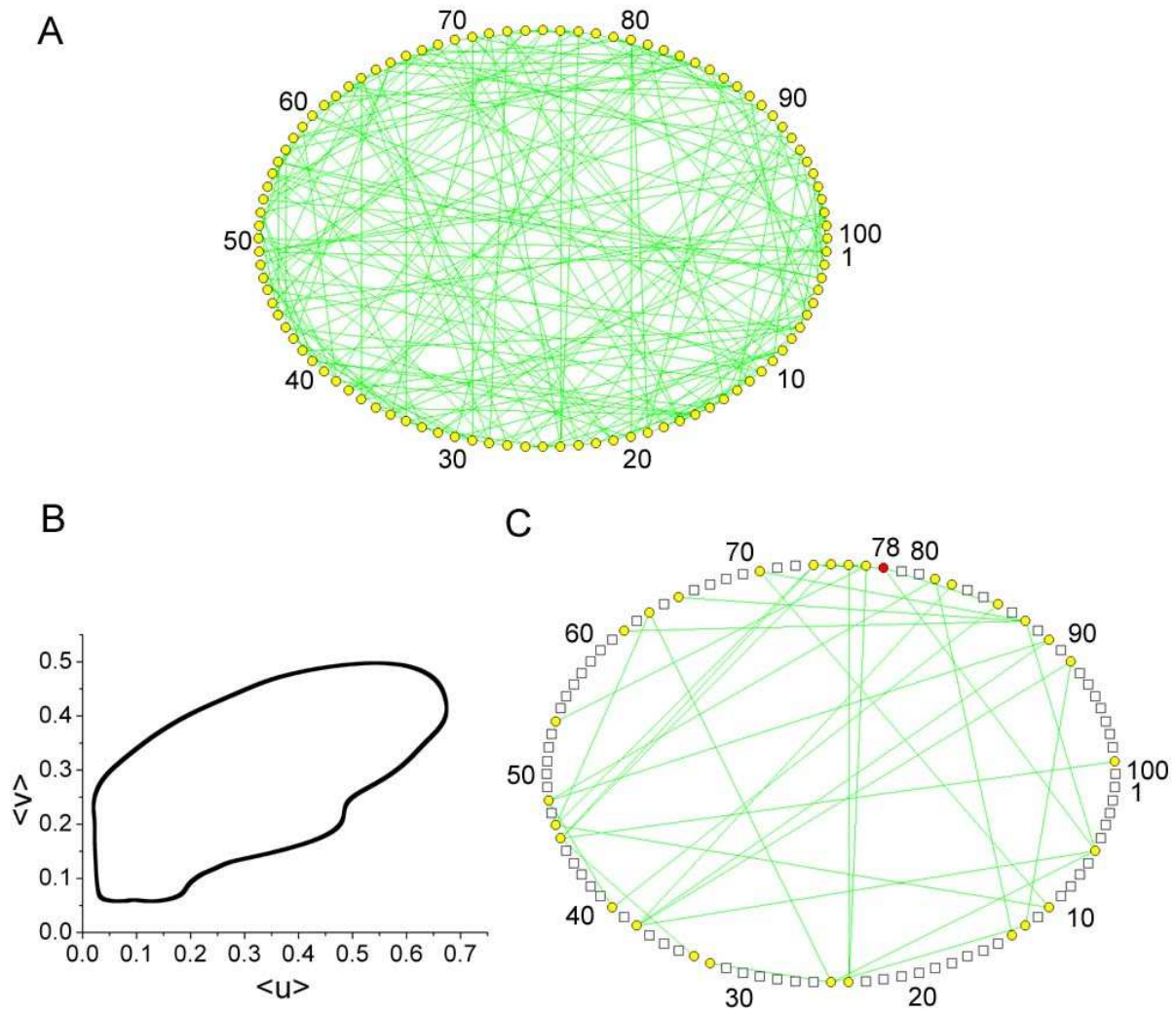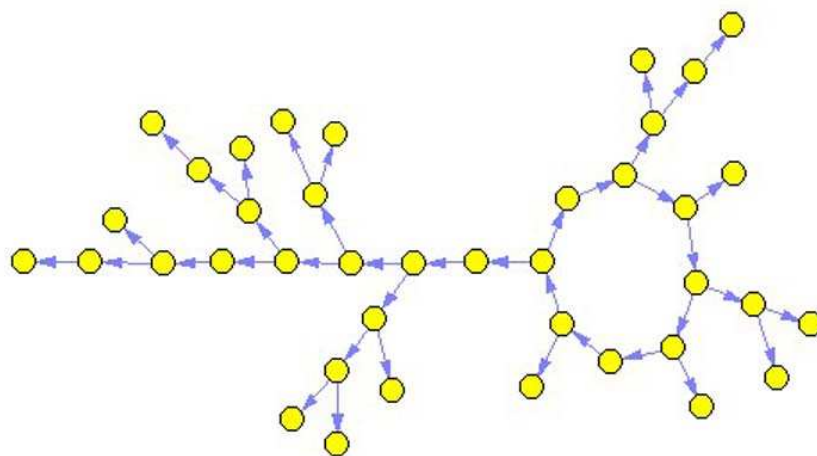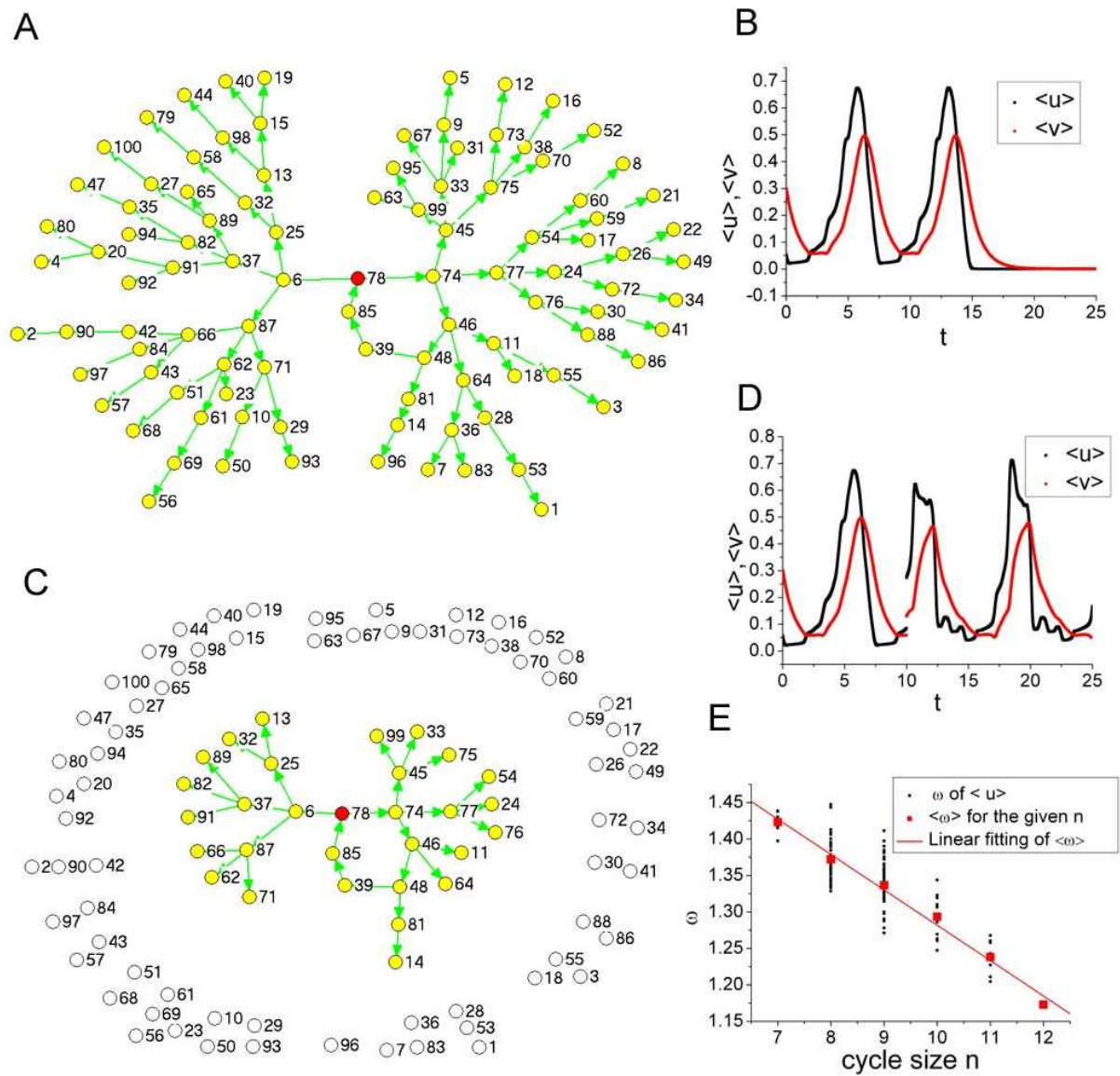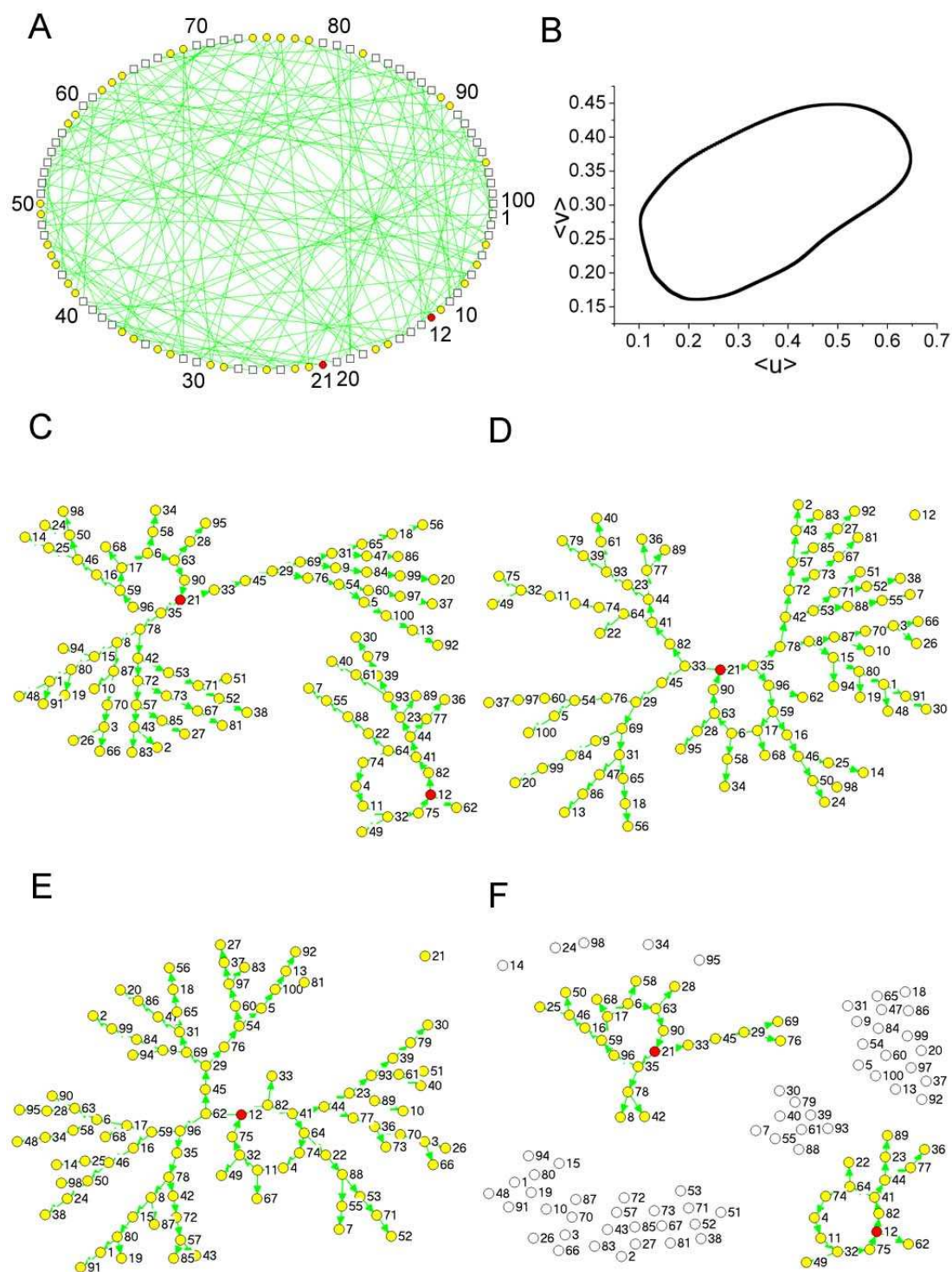
A

B

C

Fig. 1

Fig. 2

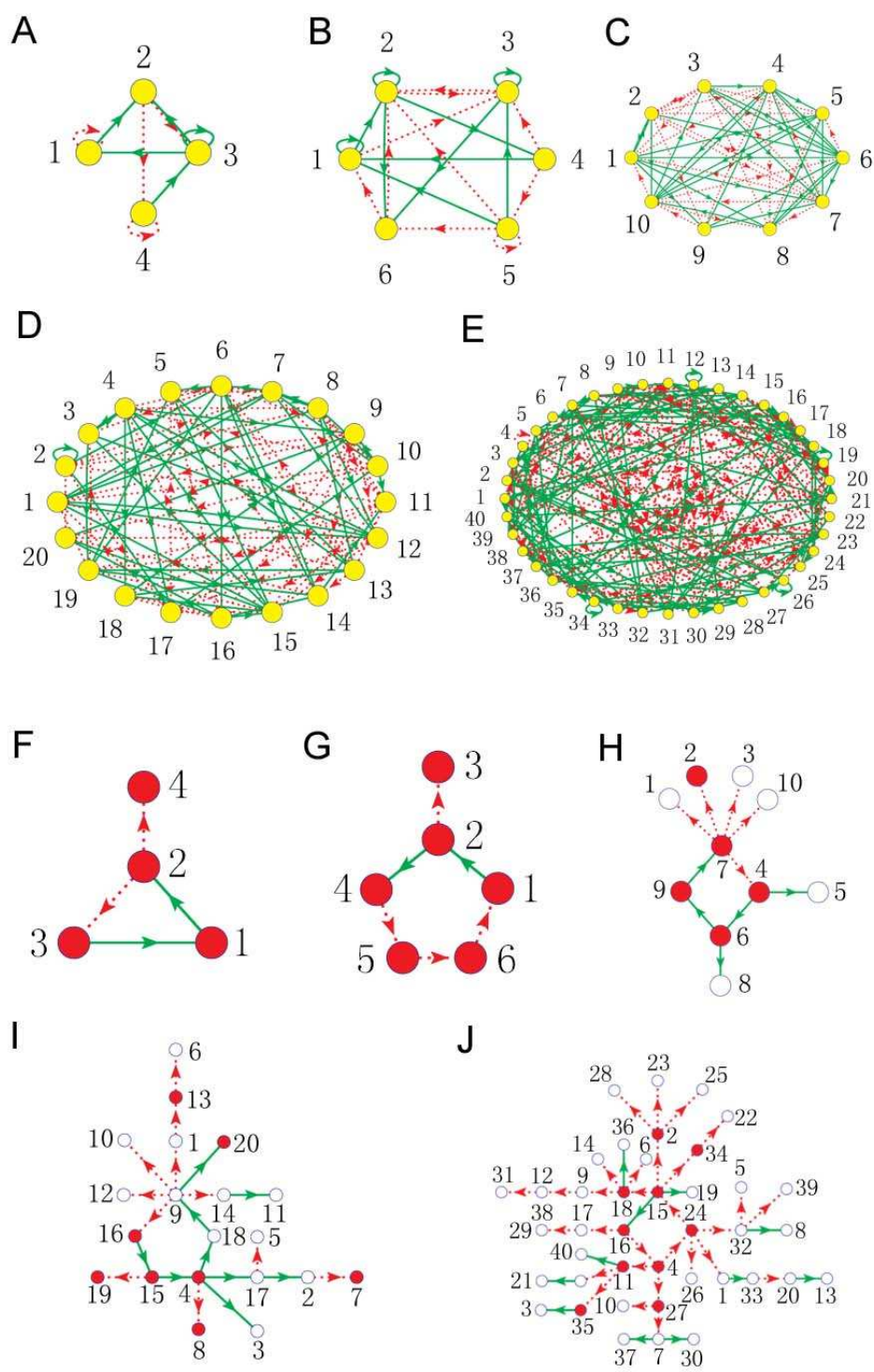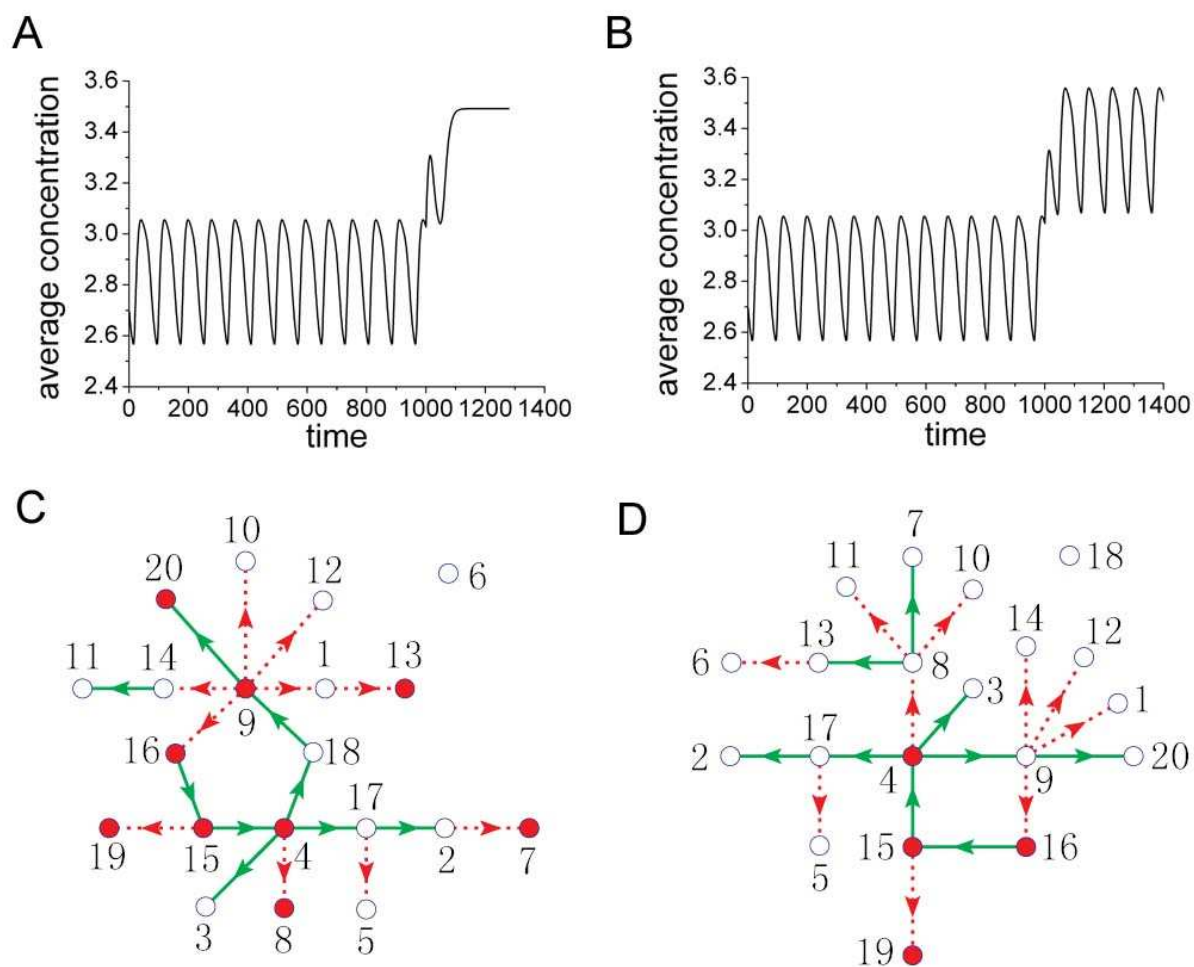Fig. 3

Fig. 4

Fig. 5

A

B

C

D

Fig. 6

Supplementary Information

Part 1 Oscillatory excitable cell networks with random symmetric interactions

We have investigated a large number of different ECN. First, we have tested ECNs of Eqs.(1) for different random coupling structures, different random initial conditions and different system sizes. From these tests we found many oscillatory configurations. For each oscillatory network we drew the dominant phase-advanced interaction pattern, and found that all patterns show BC structures of type Fig. 2.

In Fig. S1A we show an interaction structure of an ECN with $N = 200$, $\nu = 3$ and $D_u = 1.0$, which is periodically oscillatory for certain initial conditions. Though the random interaction network looks even more complicated than Fig. 1A, the reduced BC patterns are still simple and instructive. In Figs. S1B-D we show three different BC patterns for three given initial conditions. These oscillations can be terminated by removing only one or two key red circle nodes (e. g. node 30 for Fig. S1B, nodes 6 and 38 for Fig. S1C; and nodes 126 and 178 for Fig. S1D). A particular case is Fig. S1D where the BC pattern has a single long 4π circle consisting of 21 cells (by $2k\pi$ circle we mean that phase angle variation in the circle is $2k\pi$ with wave number k). Now we can't suppress oscillations by removing a single cell. Instead, a pair of cells with phase angle distance about 2π should be removed simultaneously. In all the three cases of Figs. S1B-D oscillations can persist and BC circles cannot be slightly changed after 70% nodes (all at the end of branches) are removed simultaneously. One of these results is given in Fig. S1E. It is noticed that in Figs. S1B-D the nodes immediately upstream to each red node, provide the only phase-advanced interactions for the corresponding red nodes. Therefore, removing the nearest upstream node of any red node is equivalent to remove this downstream red node.

In Fig.S2 we show interesting BC pattern manipulations when oscillations are not terminated by removing some key nodes. In Fig. S2A(S2B) we remove a red cell 6 (38) from Fig. S1 C, and find that the up-left (low-right) BC circle is destroyed while the other remaining

circle serves as the only source circle in the new BC pattern. In Fig. S2C (S2D) we remove a single red node 126 (red node 178) from Fig. S1D. Now we find that the BC circle shrinks from the 4π circle to a 2π loop with the key node 178 (key node 126) serving as the key circle node in the new BC structure. Pictures of Figs. 4 and S2 show various structure reorganizations by controlling few key nodes recognized from the BC patterns. On the other hand, oscillations are insensitive to the control of various branch nodes.

In Fig. S3 we plot various BC patterns for networks with even larger sizes. In Figs. S3A-C we take $N = 400$ for different interaction structures and different initial conditions. We find BC patterns with a 2π circle (A), 4π circle (B), and two 2π circles (C), respectively. The numbers inside the circles indicate the indexes of the circle nodes while those outside the circles associated with arrows denote the size of branches rooted at the given circle nodes. In Figs. S3D-F we do the same as Figs. S3A-C by taking $N = 2500$. Now the network size is many times larger than Fig. 1A. However, the prediction of the universal BC structure of Fig. 2 is still verified perfectly. An interesting phenomenon is that we find triple BC clusters in Fig. S3F.

The BC pattern analysis can be extended to complex networks of neural cells. Let us consider the network of FHN model(1,2)

$$\frac{du_i}{dt} = \frac{1}{\varepsilon}\left(u_i - \frac{u_i^3}{3} - v_i\right) + D_u \sum_{j=1}^{\nu}(u_{ij} - u_i) \ ,$$

$$\frac{dv_i}{dt} = \varepsilon(u_i + \beta - \gamma v_i), \qquad i = 1, 2, ..., N \qquad (S1)$$

which has been extensively used to describe neural dynamics. For the given parameter set given here the individual neural cells are excitable while nonoscillatory. For certain initial preparations the network of coupled cells can be self-organized to sustained oscillations. Fig. S4A shows one of such network and Figs. S4B and 4C present two different periodic orbits of the same network structure in Fig. S4A for two sets of different initial conditions. Figs. S4D and S4E present the BC patterns corresponding to states Figs. S4B and S4C, respectively. The one circle (Fig. S4D) and two circle (Fig. S4E) BC structures are identified by applying the CR method.

Part 2 Oscillatory dynamics of genomic regulatory networks of Eqs. (2)

Firstly, the oscillatory negative feedback loops(NFLs) of GRNs for $q \leqslant 5$ are presented in Fig. S5.

In order to define phase-advanced interactions of Eqs. (6) and (7), we should first specify the meaning of phase ϕ_i with Fourier decomposition. With ϕ_i known, the phase of interaction from node j to node i (denoted by $\phi_{j\to i}$) can be identified by ϕ_j ($\phi_j+\pi$) for positive (negative) interaction, and the interaction with $0 \lesssim \phi_{j\to i} - \phi_i \lesssim \frac{\pi}{2}$ is called phase-advanced driving. For defining the dominant phase-advanced driving of a given node i, we should identify the interaction with the maximum amplitude among all the phase-advanced interactions of node i.

The phase of single node i can be define as follows:

$$sin\phi_i = \frac{\beta_i}{\sqrt{\alpha_i^2 + \beta_i^2}}, \qquad cos\phi_i = \frac{\alpha_i}{\sqrt{\alpha_i^2 + \beta_i^2}}, \qquad (S2)$$

$$\alpha_i = \frac{2}{T}\int_0^T \Delta x_i sin(\frac{2\pi t}{T})dt, \quad \beta_i = \frac{2}{T}\int_0^T \Delta x_i cos(\frac{2\pi t}{T})dt,$$

$$\Delta x_i = x_i(t) - \overline{x}_i, \qquad \overline{x}_i = \frac{1}{T}\int_0^T x_i(t)dt, \quad i = 1, 2, \cdots, N.$$

Suppose $A_{j\to i}(t)$ is the interaction from node j to node i which can be computed explicitly by linear approximation as

$$A_{j\to i}(t) = \frac{\partial f_i}{\partial x_j}\Delta x_j, \qquad (S3)$$

where $\frac{\partial f_i}{\partial x_j}$ is a constant valued at time averages $\overline{x}_k$ ($k = 1, 2, \cdots, N$). $A_{j\to i}(t)$ is periodically oscillatory with period T and zero average. With Eqs. (S2) (S3) the phase $\phi_{j\to i}$ can be define by ϕ_j ($\phi_j + \pi$) for positive (negative) interaction, and the amplitude of $A_{j\to i}(t)$ is given by

$$\|A_{j\to i}\| = \|\frac{\partial f_i}{\partial x_j}\|\sqrt{\alpha_j^2 + \beta_j^2}, \qquad (S4).$$

The dominant phase-advanced driving of node i is the interaction with the largest amplitude $\|A_{j\to i}\|$ among all the phase-advanced interactions of node i (i.e, all j s with $0 \lesssim \phi_{j\to i} - \phi_i \lesssim \frac{\pi}{2}$).

The crucial point of the approximations of Eqs. (S2)-(S4) is to neglect the contributions of all high-frequency harmonics of the interactions and thus the definitions work very well for the cases of single-peaked periodic motions. Some slight modification is needed if the motion is multiple-peaked, and these cases are not considered in the present article. It happens with extremely low probability that the sum of interactions of a given node obeys the driving condition Eq. (7) while individual interactions do not. In this case we simply define the interaction with phase nearest to the region as the dominant interaction. These cases occur always (with our observations) for the nodes near the branch ends.

Part 3 Oscillatory dynamics of genomic regulatory networks of type "OR" interactions

Eqs. (2) consider "AND " type of joint regulations of activatory and repressive regulators, represented by the productive formula. In realistic regulatory networks there also exist joint regulations of type "OR ". Typical mathematical formulas of a network of this type (3,4) with size N are as follows:

$$\frac{dx_i}{dt} = \gamma_i(1 - x_i) + \sum_{j=1}^{N} f_{ij} , \qquad i = 1, 2, \cdots, N , \qquad (S5)$$

$$f_{ij} = \begin{cases} 0 & \text{no coupling ,} \\ (1 - x_i)\dfrac{k_{ij}\, x_j^{h_i}}{K_i^{h_i} + x_j^{h_i}} & \text{positive coupling ,} \\ -x_i\dfrac{k_{ij}\, x_j^{h_i}}{K_i^{h_i} + x_j^{h_i}} & \text{negative coupling .} \end{cases}$$

Both Eqs. (2) and (S5) are approximations of more realistic as well as more complicated regulatory networks mixing "AND" and "OR" dynamics.

Since in Eqs. (S5) each node does not oscillate individually and positive (negative) regulations tend to increase (reduce) monotonously the concentration of the protein interacted,

the phase relations analyzed in the article, are satisfied entirely. In particular, the phase and amplitude of couplings are given by Eqs. (6) and (S4), respectively, with f_i replaced by $\sum_{j=1}^{N} f_{ij}$. For mathematical simplicity we again take identical parameters in Eqs. (S5) for all nodes $h_i = h$, $k_{ij} = k$, $K_i = K$, $i = 1, 2, \ldots, N$, except $\gamma_{i=1,\ldots,N-1} = \gamma$, $\gamma_N = 1.0$.

In Figs. S6 we do the same as Fig. 5 with Eqs. (2) replaced by the "OR" dynamics of Eqs. (S5). It is really striking that though the coupling dynamics of Eqs. (S5) is different from that of Eqs. (2) considerably, BC patterns of Eqs. (S5) have essentially the same structures as Fig. 5, and all the features predicted in Fig. 2 are confirmed perfectly in Fig. S6. Moreover, the prediction of oscillation sources (one of the oscillatory NFLs in Fig. S5) is also fully verified by all the BC circles obtained from Eqs. (S5). We have also made statistics of the circuits of Eqs. (S5) with huge number of tests by varying coupling structures, parameter values and initial conditions (10^6 for 3-node, 10^4 for 4, 5-node, 10^3 for 10, 20-node). We find that the predictions on BC structures in Fig. 2 and Fig. S5 are well confirmed by all tests of oscillatory circuits with no exception.

References

[1] Fitzhugh R (1961) Impulses and physiological states in theoretical models of nerve membrane. *Biophys. J.* 1:445-466.

[2] Izhikevich E M (2004) Which model to use for cortical spiking neurons. *IEEE Trans. on Neural Networks* 15:1063-1070.

[3] Elowitz M B, Leibler S (2000) A synthetic oscillatory network of transcriptional regulators. *Nature* 403:335-338.

[4] Buchler N E, Gerland U, Hwa T (2003) On schemes of combinatorial transcription logic. *PNAS* 100:5136-5141.

Fig. S1. Oscillatory behaviors of a complex ECN of Eqs. (1) with $N = 200$, $\nu = 3$, $D_u = 1.0$. All other parameters are the same as Fig. 1(A). *(A)* Interaction structure under consideration. *(B)-(D)* BC patterns of periodically oscillatory states of ECN (A) for three

different initial conditions. All red nodes have the same meanings as those in article. *(B)* BC pattern with a 2π circle. *(C)* BC pattern with two source circles. In order to suppress the oscillation one has to remove the two red nodes 6 and 38 simultaneously, destroying both source circles. *(D)* BC pattern with with a 4π (wave number $k = 2$) circle of circle size $n = 21$. We find two red nodes in the circle separated by about 2π distance. In order to suppress oscillation we have to remove both red nodes 126 and 178 simultaneously. *(E)* The BC pattern constructed for the new oscillatory state after removing 140 nodes from (D). Oscillation persists and the original BC circle remains unchanged after 70% nodes are removed. Similar results (not shown) can be obtained also for BC patterns of (B) and (C).

Fig. S2. BC pattern manipulations. *(A)(B)* BC patterns after removing a red node 6 and the other red node 38 from Fig. S1(C), respectively. In both cases, the circle containing the removed node is destroyed and the remained circle serves as the unique oscillation source of the network. *(C)(D)* BC patterns with red nodes 126 and 178 removed from Fig. S1(D), respectively. Now the 4π BC circle of Fig. S1(D) shrinks to a 2π circle with the remaining red node being the key circle node in the new BC pattern.

Fig. S3. BC patterns of Eqs. (1) for different system sizes with $\nu = 3$, $D_u = 1.0$. All other parameters are the same as Fig. 1(A). Interaction structures and initial conditions are chosen randomly. *(A)-(C)* BC patterns with $N = 400$ for different states. Numbers inside the circle indicate the corresponding indexes of corresponding nodes, and the numbers outside the circle, associated to circle nodes by arrows, denote the sizes of the branches rooted at the given nodes. All nodes without arrows have no downstream branch. Single 2π BC circle; single 4π circle and double-circle structure are observed in (A)(B)(C), respectively. *(D)-(F)* The same as (A)-(C) with $N = 2500$. Single-, double- and triple-circle BC structures are identified in (D)-(F), respectively.

Fig. S4. Oscillatory complex network of FHN cells (Eqs. (S1)) and some examples of BC patterns. The parameters are set as $\varepsilon = 0.2$, $\gamma = 0.5$, $\beta = 1.0$. All couplings with coupling strength $D_u = 0.1$ are randomly chosen between N nodes each having coupling degree ν. *(A)* An example of FHN network with $N = 100$, $\nu = 3$. *(B)(C)* Two periodic orbits of network (A) for two different initial conditions. *(D)(E)* The BC patterns corresponding to the states (B) and (C), respectively. The red nodes have the same meanings as Figs. 3(A)

and 4(C).

Fig. S5. All oscillatory q-node NFLs of Eqs. (2) for $q \leq 5$. The solid green (red dashed) line denotes positive (negative) regulation. *(A)* 2-node NFL. *(B)* 3-node NFL with three negative interactions. *(C)* 3-node NFL with a single negative interaction. *(D)* 4-node NFL with three negative interactions. *(E)* 4-node NFL with a single negative interaction. *(F)* 5-node NFL with a single negative interaction. *(G)* 5-node NFL with three negative interactions (Type I). *(H)* 5-node NFL with three negative interactions (Type II). *(I)* 5-node NFL with five negative interactions. All these oscillatory NFLs have been observed in various BC patterns.

Fig. S6. Numerical results on oscillatory GRNs of Eqs. (S5) (type "OR"). Homogeneous parameter sets are used with $h_i = h$, $k_{ij} = k$, $K_i = K$, $i = 1, 2, \ldots, N$, except $\gamma_{i=1,\ldots,N-1} = \gamma$, $\gamma_N = 1.0$. We use two sets of parameters in simulation. In Figs. (F), (G), (J) $h = 3$, $k = 734.5525513$, $K = 3.5531352$, $\gamma = 0.8991836$; in Figs. (H), (I) $h = 4$, $k = 753.6924438$, $K = 0.6794546$, $\gamma = 0.1966502$. These parameters are randomly taken in the available ranges specified in Science report (3). In all systems unique periodically oscillatory solutions are asymptotically approached from arbitrary initial conditions. *(A)-(E)* Interaction structures of GRNs of different size N and different number I of interactions. *(A)* $N = 4$, $I = 9$. *(B)* $N = 6$, $I = 28$. *(C)* $N = 10$, $I = 56$. *(D)* $N = 20$, $I = 109$. *(E)* $N = 40$, $I = 222$. *(F)-(J)* BC patterns corresponding to (A)-(E), respectively. Red and empty nodes have the same meanings as in Figs. 5 (F)-(J).
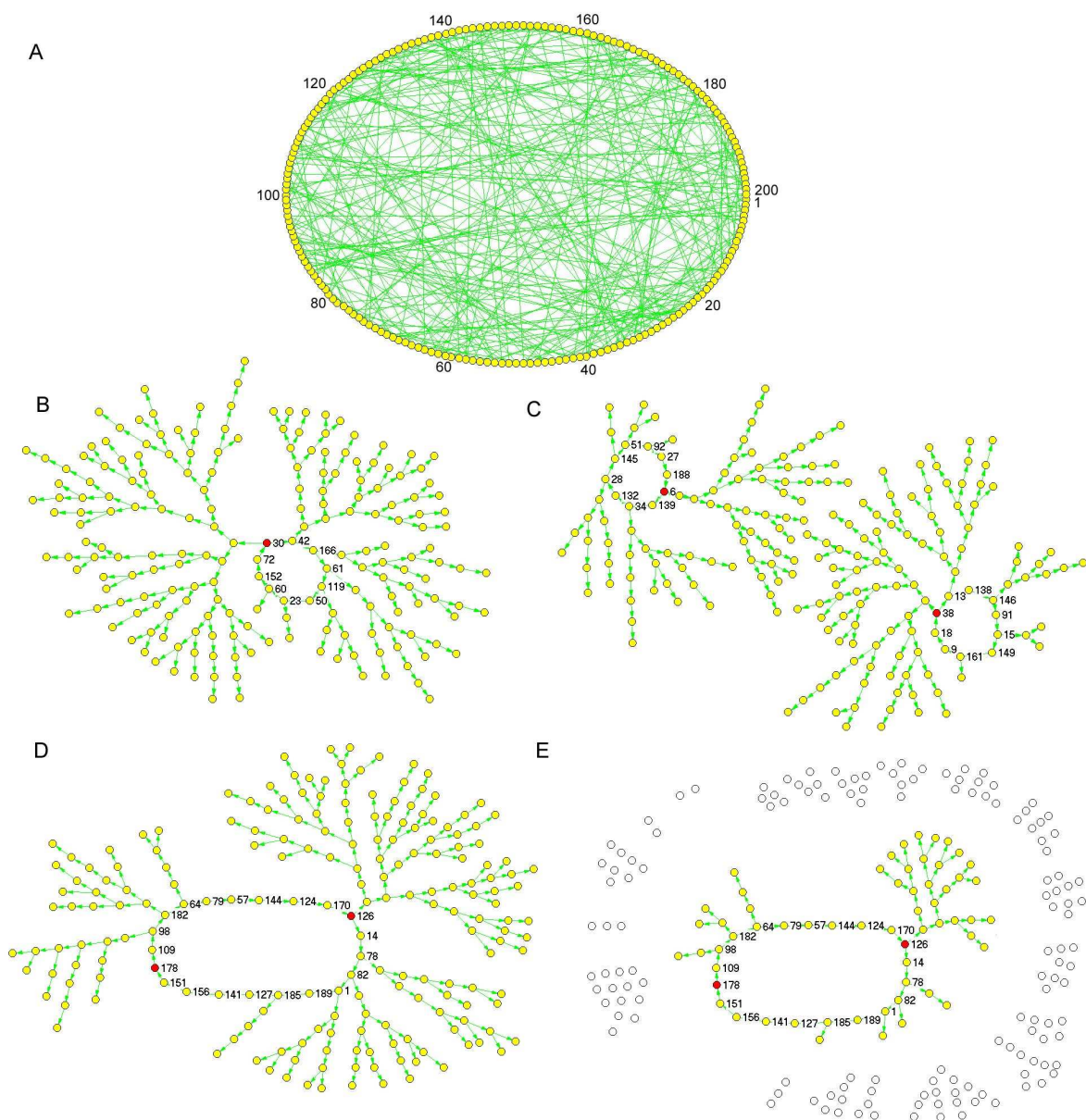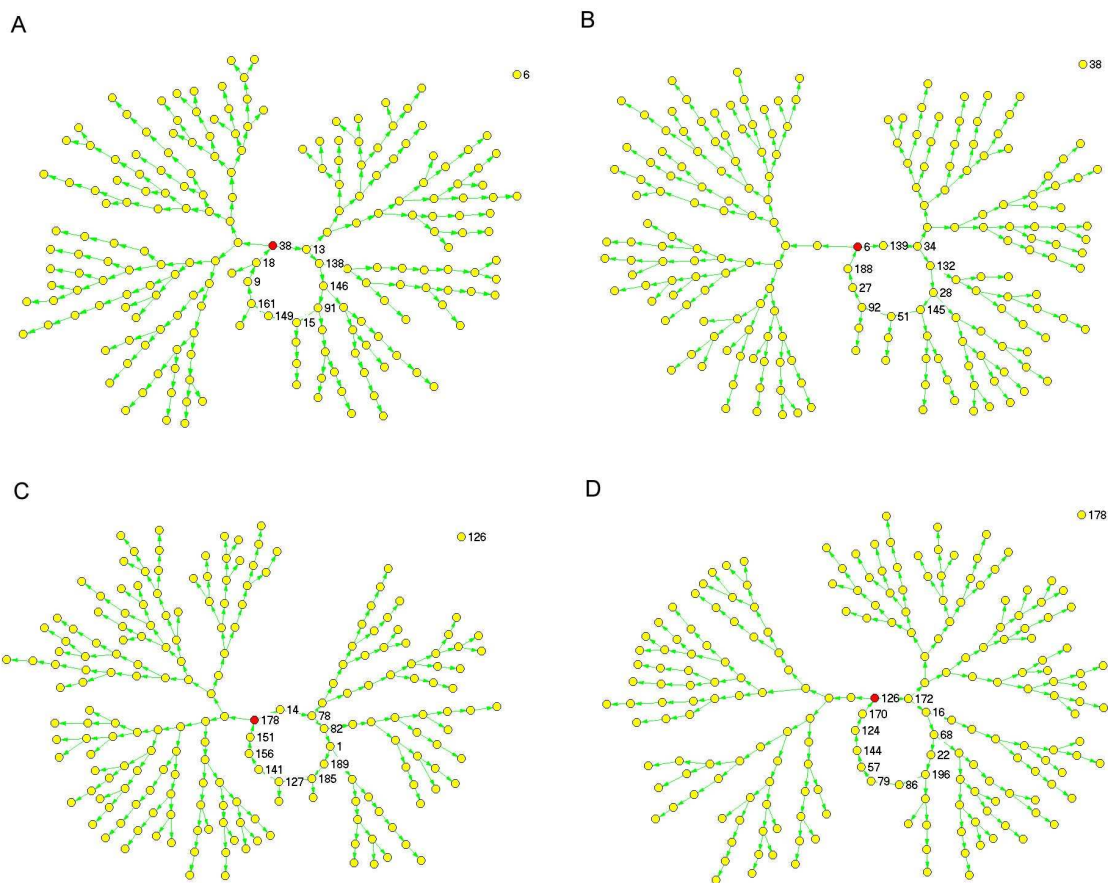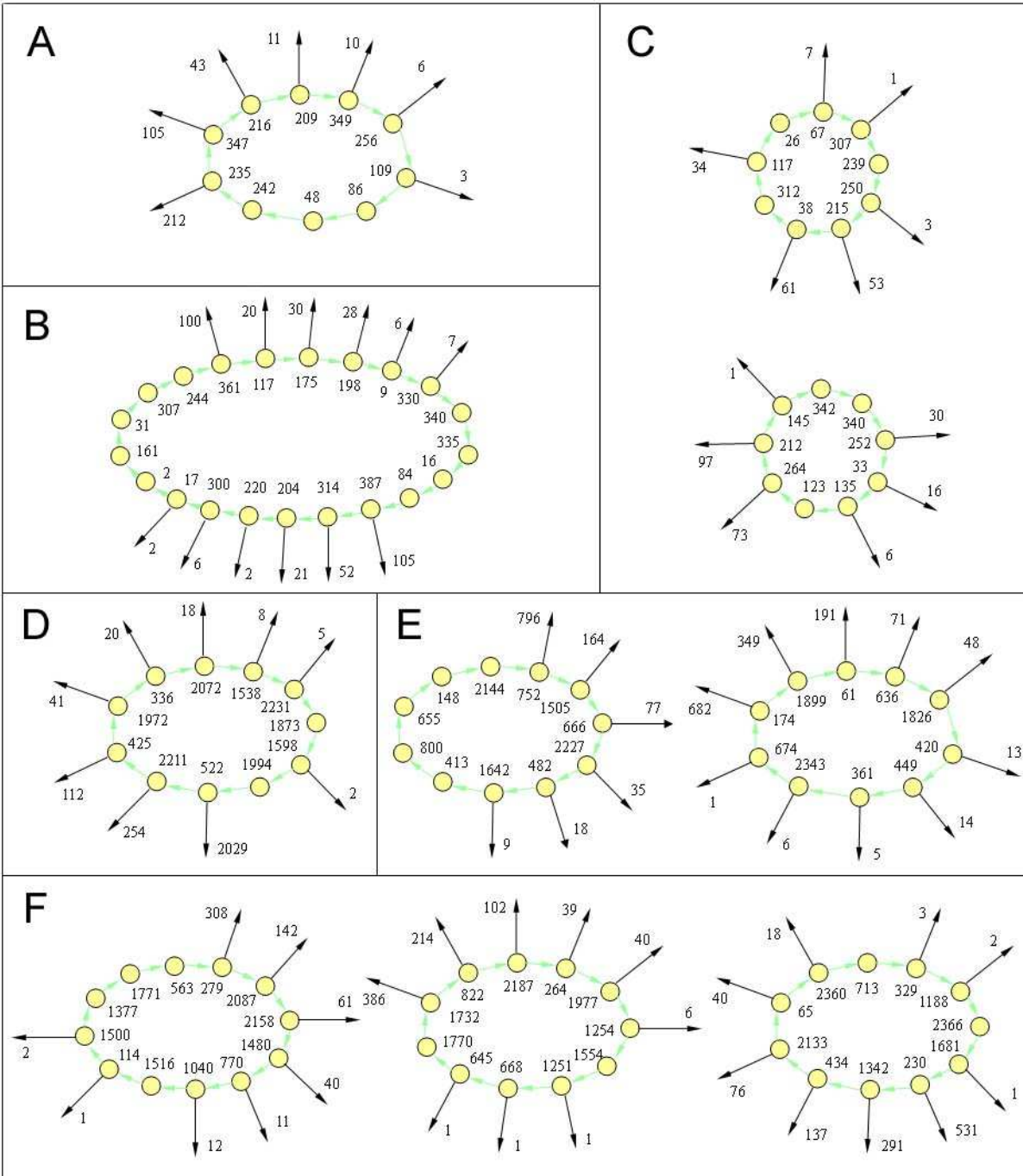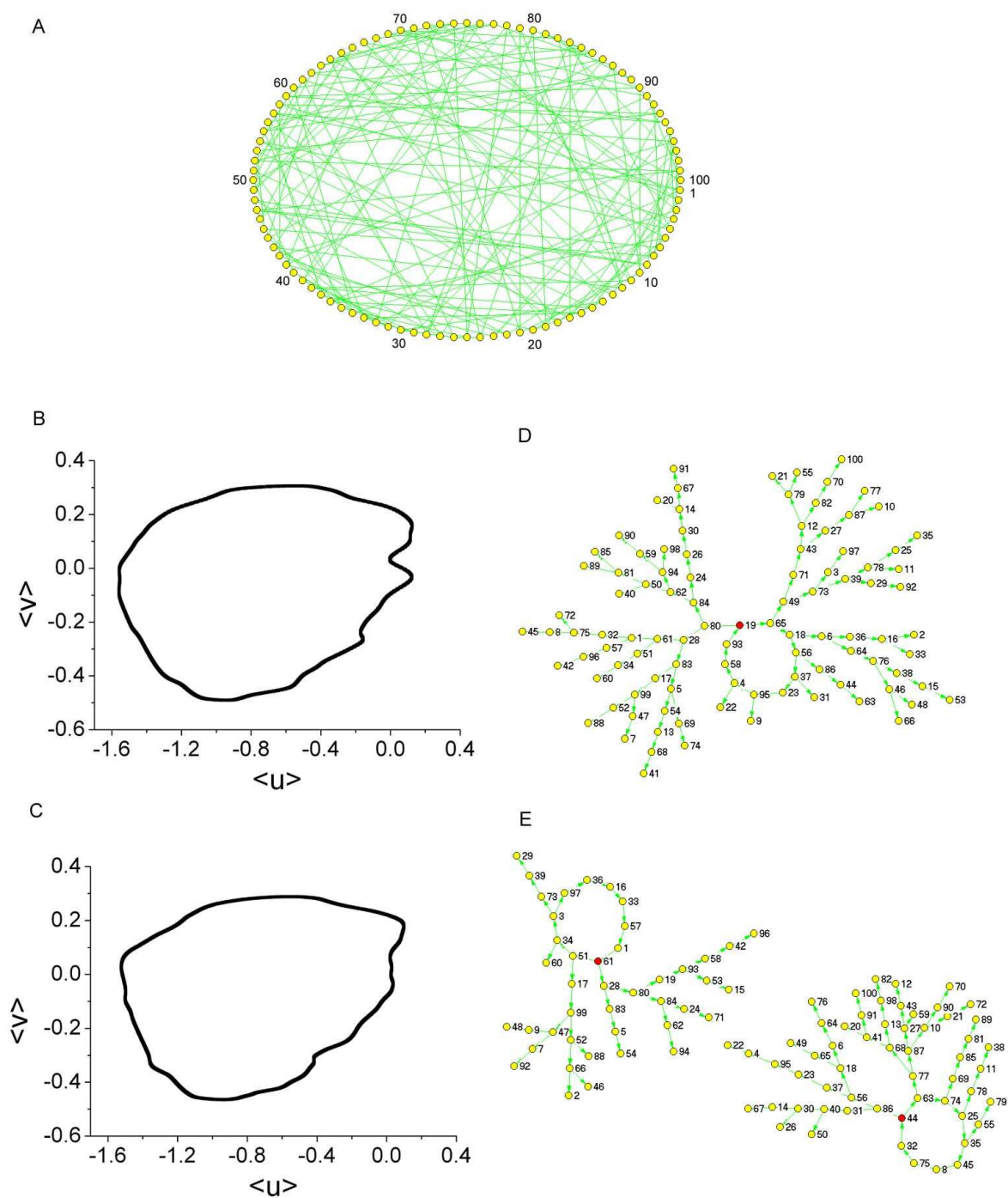
Fig. S1

A

B

C

D

Fig. S2

Fig. S3

Fig. S4

Fig. S5

A B C

D E

F G H

I J